PLASTIC STRAIN ANALYSIS OF HEAT EXCHANGER TUBESHEETS

H. GIESECKE, J.C. NICHOLS,

MPR Associates, Inc., Washington, DC

A. LOHMEIER,

Westinghouse Electric Corporation, Power Systems, Tampa, Florida, U.S.A.

ABSTRACT

In recognition of the validity of plastic strain analysis in evaluating pressure vessel structures, recent revisions to the ASME Boiler and Pressure Vessel Code - Section III - Class A Nuclear Vessels have permitted use of this technique in demonstrating compliance with Code rules. The limit pressure of complex structures obtained through plastic strain analysis provides a more meaningful datum on which to measure safety factor than the conventional comparison of local stress intensities with allowable values.

A plastic strain analysis technique has been devised for application to a common heat exchanger configuration - a tubesheet connected at its outer periphery to a spherical shell on one side and a cylindrical shell on the other. The technique is based on shell theory and interaction analysis with appropriate modifications in the plastic regions of the structure. Simplified yield conditions developed by Hodge for sandwich plates and shells of perfectly elastic-perfectly plastic material are applied and solutions yield tubesheet and shell strains and deflections over the applied pressure path as well as the limiting pressure of the structure.

Due to scarcity of applicable experimental results of strains and deflections of vessels containing flat plates welded to spherical and/or cylindrical shells under pressure, a fully instrumented steel model was constructed and pressurized well into the plastic region while deflections and strains were recorded. Analysis results were compared to the model test results and found in good agreement. Furthermore, similar corroboration is shown from comparison with tests by Marcel Save and short cylinders enclosed with circular flat plates. The good agreement in both cases allows useful application of plastic strain analysis techniques for heat exchanger tube sheet structural evaluation.

1. INTRODUCTION

In recognition of the validity of plastic strain analysis in evaluating pressure vessel structures, recent revisions to the ASME Boiler and Pressure Vessel Code - Section III - Class A Nuclear Vessels [1] have permitted use of this technique in demonstrating compliance with Code rules. The limit pressure of complex structures obtained through plastic strain analysis provides a more meaningful datum on which to measure safety factor than the conventional comparison of local stresses with allowable values.

A plastic strain analysis technique has been devised for application to a common heat exchanger configuration -- a tubesheet connected at its outer periphery to a spherical shell on one side and a cylindrical shell on the other (Figure 1). The technique is based on shell theory and interaction analysis with appropriate modifications in the plastic regions of the structure. Simplified yield conditions developed by Hodge [2] for sandwich plates and shells of perfectly elastic - perfectly plastic material are applied and solutions yield tubesheet and shell strains and deflections over the applied pressure path as well as the limiting pressure of the structure.

The agreement of values of strains and deflections calculated by the plastic strain analysis technique with experimental values of strain and deflection has been good. The experimental values of strain and deflection in the plastic region include results from a fully instrumented limit model tested under over-pressure conditions at the Westinghouse Development Engineering Laboratory at South Philadelphia, and deflections as a function of pressure which have been reported by Marcel Save [3] for a short cylinder closed by a circular flat plate.

2. ANALYTIC APPROACH

The plastic analysis technique developed for the plastic strain analysis handles any combination of circular flat plates (perforated or unperforated), cylindrical shells, and hemispherical heads. The calculation approach and derivations of basic equations utilized by the plastic analysis technique are described in detail in the Appendix.

Assumptions in the computational procedure consider ideally elastic-plastic material, neglecting strain hardening. The cross section of any portion of the structure is totally elastic with respect to bending until the full yield moment is experienced at that section, after which the cross section is considered fully plastic. Yielding is determined by the Tresca Yield Criteria. Furthermore, deformations are assumed sufficiently small that membrane forces do not support the structure against further transverse deformation in circular flat plates and axial deformation in shells. Plastic zones spreading axially in spherical shells are determined from approximation as cylindrical shells of the same radius and thickness, requiring that the plastic zones remain localized near the equatorial region of the hemispherical head.

For the interaction analysis, the structure is divided into parts consisting of a circular flat plate, cylindrical shell, and hemispherical head. Equilibrium equations for each element are written in terms of stress resultant bending moments, membrane, and shear forces.

Compatibility requirements lead to similar equations for the strain components. The resulting differential equations are then integrated either by specifying a relation between stress and strain components or by requiring stress components to exist on the yield polygon. For the elastic region, the relation between stress and strain components is provided by Hooke's Law. In the plastic region, the yield condition requires stress components to be on the yield polygon and the equilibrium equation is integrated directly. Strain components are determined from stress components by integrating strain rates over the pressure load path.

The above procedure results in equations for stress and strain components in terms of integration constants which are evaluated by imposing continuity requirements on deformations and stress resultants acting between parts of the structure.

Where plastic zones occur in the structure, the computational procedure provides for addition of a new section which is assumed entirely plastic, the length of which is equal to the extent of the plastic zone. The zone length becomes an additional unknown and is determined by requiring the yield condition to be continuous at the zone edge. The equations are nonlinear in terms of zone length and are solved analytically (in the case of the flat plate) or by trial and error convergence procedure (in the case of the cylindrical shell). The iterative procedure requires machine computation for which a computer program LIMIT was written.

3. COMPARISON WITH EXPERIMENTAL RESULTS

Due to scarcity of applicable experimental results of strains and deflections of vessels containing flat plates welded to spherical and/or cylindrical shells under internal pressure, a fully instrumented steel model (Figure 1) was constructed and pressurized well into the plastic region while deflections and strains were recorded. Dial indicators were used to indicate tubesheet deflection and strain gages were appropriately located to record strains on the circular plate surfaces and at the juncture of cylindrical and spherical shells with the circular plate. High strain region strain gage readings were corroborated with Photostress readings at the shell-plate junctures. These measured values of strain and deflection were then compared with the values of strains and deflections calculated by the LIMIT computer program.

Measured and calculated strains on the circular flat plate are plotted against pressure in Figure 3. Measured and calculated deflections of the circular flat plate are plotted in Figure 2. The limit pressure predicted by the computer program for the model was 2410 psi. The agreement between measured and calculated strains and deflections is considered good up to the predicted limit pressure.

In addition, Marcel Save [3] has reported the results of limit test on a number of shapes, including short cylinders closed with relatively thick circular flat plates. The deflections of the center of the circular flat plate measured by Save as a function of pressure are compared in Figure 4 with deflections calculated by the plastic limit analysis program. The calculated limit pressure for this configuration is 1110 psi. Again, the agreement between calculated and measured deflections is considered to be good.

4. CONCLUSION

In summary, the good agreement between measured and calculated strains and deflections on the test models allows useful application of plastic strain analysis techniques for heat exchanger tubesheet evaluation. As a point of interest, the running time for prediction of strains, deflections and limit pressure for the model shown in Figure 1 and which are plotted in Figures 2 and 3 is less than 30 seconds on the CDC 6600 computer.

5. ACKNOWLEDGEMENT

The test of the model used to obtain measured stresses and deflections was conducted at the Westinghouse Steam Division Development Engineering Laboratories under the technical direction of Mr. T. Bowes of the Development Engineering Laboratory and Mr. R. P. Biggers of MPR Associates. Meticulous attention to detail was required to ensure that valid and usable test results were obtained.

6. REFERENCES

[1] American Society of Mechanical Engineers Boiler and Pressure Vessel Code, Section III - Nuclear Vessels, New York, 1968.

[2] Hodge, Phillip G., Limit Analysis of Rotationally Symmetric Plates and Shells, Prentice Hall, New Jersey, 1963.

[3] Save, Marcel, "Experimental Verification of the Plastic Limit Analysis of Plates and Shells in Soft Steel," Publication of the Center of Scientific and Technical Researches of the Industry of Metal Fabrications, Brussels, February, 1966.

[4] Tekinalp, Bekir, Elastic-Plastic Bending of a Built-In Circular Plate Under a Uniformly Distributed Load, Journal of the Mechanics and Physics of Solids, 1957, Vol. 5, pp 135 to 142.

APPENDIX

DERIVATIONS AND CALCULATIONAL PROCEDURE

1. NOMENCLATURE

w	Normal displacement	M	Bending moment
u	In-plane displacement	N	Membrane force
k	Curvature	Q	Shear force
x	Axial distance variable	ν	Poisson's ratio
r	Radial distance variable	E	Young's Modulus
ϕ	Angular variable	t	Thickness
μ	Midsurface	R	Specific radius
e	Strain	L	Specific length
σ	Stress	ρ	Extent of a plastic zone
P	Pressure	α	An integration constant
ω	Generalized displacement	λ	Strain rate vector
C	Structural coefficients	A	Interaction matrix
z	A function of x	B	Yield Continuity matrix
σy	Yield stress	F	Interpolation Matrix
		Δ	Continuity difference

$D = \dfrac{Et^3}{12(1-\nu^2)}$ Flexural rigidity

$D_n = \dfrac{Et}{(1-\nu^2)}$ Longitudinal rigidity

$\beta = \sqrt[4]{\dfrac{3(1-\nu^2)}{(Rt)^2}}$ Elastic cylinder constant

$N_o = \sigma_y t$ Yield membrane

$\gamma = \sqrt{\dfrac{2}{Rt}}$ Plastic Cylinder constant

$m = \dfrac{M}{M_o}$ Reduced moment

$n = \dfrac{N}{N_o}$ Reduced membrane force

$M_o = \dfrac{\sigma y t^2}{4}$ Full yield moment

2. DERIVATION OF STRESS AND STRAIN COMPONENTS

The solution of the elastic-plastic problem discussed previously assumes the structure is divided into a number of regions, each of which is totally elastic or totally plastic with respect to a specific yield condition. There is a specific set of equations for each region giving the stress and strain components in that region. These equations are in terms of a set of constants of integration which can be determined by continuity requirements between regions.

The stress and strain components for a specific region of a circular plate or cylindrical shell are derived from equilibrium and compatibility equations for the plate or shell element. For elastic regions, Hooke's Law is used to provide an integrable set of differential equations. For plastic regions there are specific yield conditions which provide for direct integration of the equilibrium equations. Strain components can be written in terms of strain rate satisfying compatibility and integrated over the pressure load path to obtain plastic strain components. The method used to obtain strain rates and deflections for individual shapes follows the approach described by Hodge [1] .

a) Shells

A typical shell region in the structure is subjected to edge loading and internal pressure as shown in Figure 5. Since the axial stress component is invariant with x, a two dimensional polygon may be assumed whose shape and size varies as a function of n_x.

The yield condition sequences appropriate to a cylindrical shell region subjected to edge loading and pressure is illustrated in Figure 5. Stress profiles are shown for the shell with increased edge load. The size and shape of the yield polygon will be assumed constant for simplicity.

The stress profile labeled (1) corresponds to an elastic shell region. Segments OB and OI correspond to the leading and trailing edges, respectively, and the point (a) corresponds to a maximum in shell deflection where n_ϕ is also a maximum. Similarly, (b) will be a point of moment inflection on the shell. Corresponding points are labeled on the shell region in Figure 5. With increased load, the stress profile moves toward the polygon perimeter. When a point on the stress profile touches the yield polygon, plastic flow will occur at the corresponding point in the shell. For our case, this will occur first when the point A reaches point B, and yielding occurs at the shell leading edge from yield condition $m_x = -(1-n_x)$.

This yield condition cannot satisfy equilibrium over a finite shell region and a plastic region will not extend into the cylinder. Instead, a yield hinge develops at the leading edge. As loading increases, an angular discontinuity occurs at the shell leading edge and the stress profile reaches the position (2). Note that the leading edge point has moved to C, because the leading edge displacement (and n_ϕ) increases. Point C will move along the polygon with increased load toward corner D where the yield condition is $-2n_\phi + m_x = -(2+n_x)$.

This yield condition allows plastic flow over a region of the shell. Further increase in load will cause a plastic zone to spread along the shell from the leading edge. The point corresponding to the shell leading edge will remain at D. Hence, the plastic zone will spread and the yield hinge become more severe. Additional loading can cause more plastic zones to develop as shown by stress profile (4) where three different types of plastic zones and a yield hinge are present. Stress and strain component equations valid in each region are developed below from equilibrium and compatibility relations and Hooke's Law or the specific yield condition.

Equilibrium equations for a cylindrical shell are as follows:

$$\frac{dN_x}{dx} = 0 \; ; \qquad Q_x = \frac{dM_x}{dx} \; ; \qquad \frac{dQ_x}{dx} + \frac{N_\phi}{R} = P \tag{1}$$

Since N_x is not a function of x, shear can be eliminated:

$$\frac{d^2M_x}{dx^2} + \frac{N_\phi}{R} = P \tag{2}$$

The compatibility requirements for a cylinder are given in terms of the deflection, w.

$$k_x = \frac{d^2w}{dx^2} ; \qquad e_\phi = \frac{w}{R} \tag{3}$$

Using Hooke's Law in elastic region to eliminate stress components:

$$M_x = Dk_x ; \qquad N_\phi = \frac{Etw}{R} + \nu N_x \tag{4}$$

This leads to the equation for the deflection of an elastic cylinder region:

$$\frac{d^4w}{dx^4} + 4\beta^4 w = 4\beta^4 \alpha_o ; \qquad \alpha_o = \frac{(PR-\nu N_x)R}{Et}$$

The solution can be written in the following linear form:

$$w = \alpha_1 z_1 + \alpha_2 z_2 + \alpha_3 z_3 + \alpha_4 z_4 + \alpha_o \tag{5}$$

$$z_1 = \sin\beta x \sinh\beta x \qquad \frac{dz_1}{dx} = \beta(z_2+z_3)$$

$$z_2 = \sin\beta x \cosh\beta x \qquad \frac{dz_2}{dx} = \beta(z_1+z_4)$$

$$z_3 = \cos\beta x \sinh\beta x \qquad \frac{dz_3}{dx} = \beta(z_4-z_1)$$

$$z_4 = \cos\beta x \cosh\beta x \qquad \frac{dz_4}{dx} = \beta(z_3-z_2)$$

All stress and strain components are determined by the deflection or its derivatives as given in equation (1), (3), and (4), and will have linear integration constants.

To derive a similar set of equations for plastic regions of a cylinder, the yield conditions corresponding to the polygon in Figure 5 are required. These can be simplified using yield parameters ε and η which take on the values $\pm$ 1.

$$\begin{aligned} &\varepsilon m_x + \eta n_x = 1 ; && (2n_\phi - n_x) + \varepsilon m_x = 2\eta \\ &(n_\phi - n_x)\varepsilon = 1 && \varepsilon n_\phi = 1 \end{aligned} \tag{6}$$

The first corresponds to a hinge circle in the shell and results in an angle discontinuity. Regions of the shell near this point remain elastic or satisfy some other yield condition and no plastic equations are required. The other three yield conditions among equations (6) allow plastic flow to occur over a finite region of the shell. Substitution of the second yield condition into the equilibrium equation (2):

$$\frac{d^2M_x}{dx^2} - \varepsilon\gamma^2 M_x = \varepsilon\gamma^2 C_o ; \qquad C_o = \frac{\varepsilon M_o}{N_o}(-N_x+2RP) - 2\varepsilon\eta M_o \tag{7}$$

Defining a convenient set of z-functions which depend on the sign of ε:

For $\varepsilon = +1$		For $\varepsilon = -1$	
$z_1 = x\sinh\gamma x$	$z_2 = x\cosh\gamma x$	$z_1 = x\sin\gamma x$	$z_2 = x\cos\gamma x$
$z_3 = \sinh\gamma x$	$z_4 = \cosh\gamma x$	$z_3 = \sin\gamma x$	$z_4 = \cos\gamma x$

The derivatives of these functions can be expressed for either sign of ε:

$$\frac{dz_1}{dx} = z_3+\gamma z_2 ; \quad \frac{dz_2}{dx} = z_4+\varepsilon\gamma z_1 ; \quad \frac{dz_3}{dx} = \gamma z_4 ; \quad \frac{dz_4}{dx} = \varepsilon\gamma z_3$$

In terms of these functions, the solution to equation (7) becomes:

$$M_x = \bar{D}(\alpha_1 z_4 + \varepsilon\alpha_2 z_3) - C_o \;; \qquad \bar{D} = \frac{2\gamma}{4/Et^3 + 1/D} \tag{8}$$

Strain components can be found by integrating strain rates. The plastic strain rate vector is perpendicular to the yield polygon:

$$(\dot{e}^{pl}_\mu,\ \dot{e}^{pl}_\phi,\ \dot{k}^{pl}_x) = \lambda\eta(-1,\ 2,\ \frac{4\varepsilon}{t})$$

Since the total strain rates are a combination of elastic and plastic strain rates:

$$\begin{aligned}
\dot{e}_\mu &= \frac{1}{Et}(\dot{N}_x - \nu\dot{N}_\phi) - \lambda\eta \\
\dot{e}_\phi &= \frac{1}{Et}(\dot{N}_\phi - \nu\dot{N}_x) + 2\lambda\eta = \frac{\dot{w}}{R} \\
\dot{k}_x &= \frac{\dot{M}_x}{D} + \frac{4\varepsilon}{t}\lambda\eta = \frac{d^2\dot{w}}{dx^2}
\end{aligned} \tag{9}$$

Eliminating λ from the last two equations leads to the equation for plastic deflection:

$$\frac{d^2w}{dx^2} - \varepsilon\gamma^2 w = \frac{M_x}{D} - \frac{2\varepsilon}{Et^2}(N_\phi - \nu N_x)$$

From Equation (8) and the yield condition, this equation can be integrated:

$$w = \alpha_1 z_1 + \alpha_2 z_2 + \alpha_3 z_3 + \alpha_4 z_4 + \alpha_o$$

$$\alpha_o = \frac{R}{Et}(RP - \nu N_x) + \frac{C_o}{\varepsilon\gamma^2 D}$$

The axial strain at the shell mid-surface determined from equation (9) becomes:

$$e_\mu = \frac{1}{Et}\left[(\tfrac{1}{2}-\nu)\ N_\phi + (1-\frac{\nu}{2})\ N_x\right] - \frac{w}{2R}$$

The last two yield conditions among equations (6) also allows plastic flow.

$$(N_\phi - N_x)\varepsilon = N_o \;; \qquad N_\phi\varepsilon = N_o$$

Integrating equilibrium equation (2) directly and substituting into strain rate and compatibility relations:

$$w = \alpha_1 + \alpha_2 x + \alpha_3 x^2 + \alpha_4 x^3 + \alpha_o x^4$$

$$\alpha_o = \frac{PR - N_x - \varepsilon N_o}{24RD}$$

$$M_x = 2D(\alpha_3 + 3\alpha_4 x + 6\alpha_o x^2)$$

$$e_\mu = (\varepsilon N_o + 2N_x)\frac{(1-\nu)}{Et} - \frac{w}{r}$$

b) Circular Plates

The tubesheet or circular flat plate in the structure is subjected to edge loads and pressure as shown in Figure 6. The yield polygon for this loading will, in general, be a four dimensional figure, but for relatively thick plates an approach similar to that used in the shell yield polygon to eliminate N_x can be used to eliminate N_r and N_ϕ. If it is assumed that membrane stresses do not support the plate against lateral motion, the bending and membrane components of plate deformation become independent of each other and the membrane stresses can be handled separate from the bending analysis. However, the membrane stresses cannot be neglected in this analysis because of their effect on the yield polygon. With effective yield moments reduced to account for the membrane stresses in the plate, the technique employed by Tekinalp [4] can be generalized for arbitrary loading such as that given in Figure 6. The corresponding yield polygon for the circular plate yield conditions is shown in Figure 6. The polygon will reduce in size as the membrane stresses are increased. The dashed line JOAC corresponds to the plate center, since m_r must equal m_ϕ at that point. Similarly, the dashed line OBEH corresponds to the plate edge for the illustrated sequence. A typical elastic stress profile for the plate is depicted by the position labeled (1) on Figure 6. As the load is increased the stress profile will move toward the polygon perimeter such that the point A will reach the corner C, and the plate center will begin to yield due to the yield conditions at that point ($m_\phi = 1-n_\phi$; $m_r = 1-n_r$).

The second of these yield conditions cannot support plastic flow and will cause a hinge to occur at plate center. The first can be satisfied over a region of the plate. As more load is applied, a plastic zone will spread from the plate center. After additional increase in load the stress profile will assume position (2). The corner C will still correspond to the plate center and the hinge at that point will continue to become more severe. When the load becomes large enough, the point E will touch the yield polygon at H. The yield condition reached at this point is $m_\phi - m_r = 1$.

Further loading will cause a plastic zone to spread from the edge of the plate towards the center and the central zone will increase with the stress profile reaching position (3). The arc FG corresponds to an elastic annulus separating the two plastic zones given by CF and HG. The yield hinge at the plate center corresponding to point C will continue to operate.

If the initial edge moment becomes large, such as the built-in plate developed by Tekinalp [4], point H may lie below the m_r axis and a hinge may occur at the plate edge. Also, if the point D reaches corner I before point E reaches H, the secondary zone in the plate will spread outward instead of inward from the edge.

Equilibrium equations for a circular plate element are:

$$\frac{d(rM_r)}{dr} = M_\phi + rQ_r \; ; \qquad \frac{d(rQ_r)}{dr} = -P_r \; ; \qquad \frac{d(rN_r)}{dr} = N_\phi \tag{10}$$

Compatibility for small deflections requires that:

$$k_r = \frac{d^2w}{dr^2} \; ; \qquad k_\phi = \frac{1}{r}\frac{dw}{dr} \; ; \qquad e_{\mu r} = \frac{du_r}{dr} \; ; \qquad e_{\mu\phi} = \frac{U_r}{r} \tag{11}$$

For an elastic region of the plate, Hooke's Law eliminates strain components:

$$\begin{aligned} M_r &= D(k_r + \nu k_\phi) \qquad & N_r &= D_n(e_{\mu r} + \nu e_{\mu\phi}) \\ M_\phi &= D(k_\phi + \nu k_r) \qquad & N_\phi &= D_n(e_{\mu\phi} + \nu e_{\mu r}) \end{aligned} \tag{12}$$

Neglecting radial strain due to rotation in the compatibility equation for $e_{\mu r}$, membrane stress components N_r and N_ϕ and the membrane strain components $e_{\mu r}$ and $e_{\mu\phi}$ are independent of moments and curvatures of the plate.

$$\begin{aligned} N_r &= \alpha_1 + \frac{\alpha_2}{r^2} \qquad & e_{\mu r} &= \frac{N_r - \nu N_\phi}{D_n(1-\nu^2)} \\ N_\phi &= \alpha_1 - \frac{\alpha_2}{r^2} \qquad & e_{\mu\phi} &= \frac{N_\phi - \nu N_r}{D_n(1-\nu^2)} \end{aligned} \tag{13}$$

The radial deflection along the mid-surface of the plate is given by equation (11):

$$u_r = re_{\mu\phi}$$

Integrating directly for moments and curvatures:

$$rQ_r = -\frac{Pr^2}{2} + \alpha_q$$

If the plate has no central hole and the pressure on the plate is uniform ($\alpha q = 0$), substitution into the rotational equilibrium equation and use of Hooke's Law (12) results in the moments and curvatures for the elastic region.

$$M_r = \alpha_3 + \frac{\alpha 4}{r^2} - \frac{(3+\nu)}{16} Pr^2 \qquad k_r = \frac{M_r - \nu M_\phi}{D(1-\nu^2)}$$

$$M_\phi = \alpha_3 - \frac{\alpha 4}{r^2} - \frac{(3\nu+1)}{16} Pr^2 \qquad k_\phi = \frac{M_\phi - \nu M_r}{D(1-\nu^2)}$$

The rotation of the plate corss-section, given by the compatibility equation for k_ϕ, (11), can now be integrated to obtain deflection relative to that at r_o:

$$w = w(r_o) - \frac{1}{D}\left[\frac{\alpha_3}{(1+\nu)} \frac{(r_o^{\,2}-r^2)}{2} - \frac{\alpha_4}{(1-\nu)} \ln \frac{r_o}{r} - \frac{P(r_o^{\,4}-r^4)}{64}\right]$$

For a plastic region of the plate the stress components lie on the yield polygon. Using yield parameters ε and η:

$$\varepsilon\, m_r + \eta\, n_r = 1\ ; \qquad \varepsilon\, m_\phi + \eta\, n_\phi = 1\ ; \qquad \eta(m_\phi - m_r) + \varepsilon(n_\phi - n_r) = 1$$

For thick plates, membrane forces are small and plastic flow due to membrane forces is neglected; equations (13) are applicable. Moments that the plate cross-section can support are given by the yield conditions in Figure 6.

$$M_r = \varepsilon M_o(1-\frac{\eta\alpha_1}{N_o})\ ; \qquad M_\phi = \varepsilon M_o(1-\frac{\eta\alpha_1}{N_o})\ ; \qquad (M_\phi - M_r) = \eta M_o \tag{14}$$

The first condition requires a hinge and can occur only at the plate center or edge, leading to discontinuity in rotation but no finite plastic region. The second condition requires the circumferential moment to be a constant throughout the plastic zone.

$$M_\phi = \varepsilon M_o(1-\frac{\eta\alpha_1}{N_o}) \tag{15}$$

With this constant moment, the equilibrium equation (10) can be integrated directly.

$$M_r = \varepsilon M_o\ (1-\frac{\eta\alpha_1}{N_o}) + \frac{\alpha 3}{r} - \frac{Pr^2}{6} \tag{16}$$

Neglecting plastic flow due to membrane forces:

$$(\dot{k}_\phi^{pl},\ \dot{k}_r^{pl}) = \lambda(\varepsilon, 0) \tag{17}$$

The total strain rates are a combination of the elastic and plastic parts:

$$\dot{k}_r = \frac{\dot{M}_r - \nu\dot{M}_\phi}{D(1-\nu^2)} + \dot{k}_r^{pl} \qquad \dot{k}_\phi = \frac{\dot{M}_\phi - \nu\dot{M}_r}{D(1-\nu^2)} + \dot{k}_\phi^{pl} \tag{18}$$

Equation (17) implies that the radial curvature is totally elastic.

$$k_r = (M_r - \nu M_\phi)/D(1-\nu^2)$$

Use of (15) and (16) to integrate the compatibility equation results in the curvature k_ϕ:

$$k_\phi = \frac{1}{D(1-\nu^2)}\left[b\varepsilon M_o(1-\frac{\eta\alpha_1}{N_o}) + \frac{\alpha 3}{r} \ln r + \frac{\alpha 4}{r} - \frac{Pr^2}{18}\right]; \qquad b = (1-\nu)$$

Thedeflection relative to the deflection at a reference point is again solved by integrating the angle $\frac{dw}{dr} = rk_\phi$.

$$w = w(r_o) + \frac{1}{D(1-\nu^2)}\left[\frac{P(r_o^4-r^4)}{72} - (\alpha_4-\alpha_3)(r_o-r) - \alpha_3\ (r_o\ln r_o - r\ln r) - \epsilon M_o(1-\frac{\alpha_1 n}{N_o})(\frac{1-\nu}{2})(r_o^2-r^2)\right]$$

When the third yield condition among (14) is reached, moments, curvatures and lateral deflections are calculated in a similar manner. Substitution of the equilibrium equation results in a differential equation for M_r which can be integrated directly for the moments.

$$M_r = nM_o\ln r + \alpha_3 - \frac{Pr^2}{4}\ ; \qquad M_\phi = nM_o(\ln r+1) + \alpha_3 - \frac{Pr^2}{4}$$

The plastic strain rate vector for this yield condition allows plastic flow for both curvatures:

$$(\dot{k}_\phi^{pl},\ \dot{k}_r^{pl}) = \lambda(n,-n)$$

Substituting plastic strain rates into equation (18):

$$k_\phi + k_r = \frac{1}{D(1+\nu)}\ (M_r+M_\phi)$$

The compatibility equation is then used to eliminate k_ϕ or k_r.

$$k_r = \frac{1}{D(1+\nu)}\left[nM_o(\ln r+1) - \frac{3Pr^2}{8} - \frac{\alpha_4}{r^2} + \alpha_3\right]$$

$$k_\phi = \frac{1}{D(1+\nu)}\left[nM_o\ln r + \frac{\alpha_4}{r^2} + \alpha_3 - \frac{Pr^2}{8}\right]$$

The usual integration gives deflection in terms of deflection at a reference point:

$$w(r) = w(r_o) + \frac{1}{D(1+\nu)}\left[\frac{P(r_o^4-r^4)}{32} - \frac{nM_o}{2}\ (r_o^2\ln r_o - r^2\ln r) - \alpha_4\ln\frac{r_o}{r} - (\alpha_3 - \frac{nM_o}{2})\frac{(r_o^2-r^2)}{2}\right]$$

3. PROBLEM APPROACH

The difficulty in the elastic-plastic analysis of a structure requires a systematic approach for the number of variables and stress-strain relationships throughout the structure. Equations for stress and strain components can be written as linear equations in terms of their integration constants. If the structure to be analyzed is divided into axially symmetric regions, each of which is totally elastic or totally plastic, the stress and strain components in that region must satisfy one specific set of equations. Boundary constants can be determined from continuity requirements between regions. There are four integration constants for each region; hence four continuity requirements at each boundary.

For a region i, the jth component can be written:

$$\omega_j^i = \Sigma_k C_{jk}^i \alpha_k - C_{jo}^i \quad (k = 1 \text{ to } 4s) \tag{19}$$

ω_j^i only includes those components required to be continuous across boundaries of region i. The matrix C_{jk}^i depends only on the material properties and dimensions. C_{jo}^i includes all remaining terms in equation j and all pressure terms are included in C_{jo}^i. The boundary requirements now lead to a set of linear equations which can be solved for constants α_k:

$$\omega_j^i - \omega_j^{i+1} = 0\ ; \qquad \Sigma_k A_{jk}\alpha_k = A_{jo} \quad (k = 1 \text{ to } 4s) \tag{20}$$

Where: $A_{jk} = C^{i}_{jk} - C^{i+1}_{jk}$; $A_{jo} = C^{i}_{jo} - C^{i+1}_{jo}$

If a yield hinge exists at the boundary of a region, the angle equation at that point is invalid. Instead, the corresponding moment must satisfy the yield condition. The equation (20) imposed on the angle is replaced by the yield condition:

$$M_x = M_o\ (1 - \frac{N_x}{N_o})$$

In order to solve the interaction analysis described above, the length of each plastic zone must be known because the coefficient C^{i}_{jk}, and therefore the A matrix, depend on the length of the corresponding region of the structure. Let ρ_n be the length of the nth plastic zone and the yield condition continuous at edge. Since yield conditions are linear functions of stress the continuity requirement for ρ_n can be written:

$$\Sigma_j\ B_{nj}\ \alpha_j = B_{no} \tag{21}$$

The nth row of the matrix above will depend on ρ_n. It is necessary to find those values for all plastic zone lengths ρ_n which will simultaneously satisfy equations (20) and (21).

In the computer program developed, an approximation, ρ^o_n, for each zone length is supplied and the interaction analysis is solved using these approximations. Define Δ_n as a measure of how well the nth equation is satisfied:

$$\Delta_n = \Sigma_j\ B_{nj}\ \alpha_j - B_{no}$$

A variation, $\delta\rho_m$, in the plastic zone, ρ_m, will affect Δ_n as follows:

$$\delta\Delta_n = \Sigma_m\ F_{nm}\ \delta\rho_m\ ; \qquad F_{nm} = \Sigma_j\ (B_{nj}\frac{d\alpha_j}{d\rho_m} + \frac{dB_{nj}}{d\rho_m}\ \alpha_j) - \frac{dB_{no}}{d\rho_m}$$

If approximations ρ^o_n are good, differences can be made to vanish:

$$\delta\Delta_n = -\Delta_n \qquad \Sigma_m\ F_{nm}\ \delta\rho_m = -\Delta_n \tag{22}$$

These equations are solved and the zone lengths adjusted:

$$\rho_n = \rho^o_n + \delta\rho_n$$

An initial approximation for the plastic zone lengths can be found by solving the problem as if the whole structure were elastic. Regions where the elastic stress components are outside the yield polygon are then considered to be plastic and corresponding plastic zones are incorporated as initial approximations. These zones will necessarily be too small but they serve as a good starting point if the load is not too far beyond the elastic range. For loads well beyond the elastic range, an incremental loading is utilized and the initial approximations for the plastic zones at each increment are adjusted, beginning with the value found at the previous increment.

The interaction analysis is solved using the initial approximation ρ^o_n. The result is an initial set of integration constants, α^o_j. Each zone extent is then adjusted by a small value and the interaction analysis is solved again each time for new values of the integration constants. In this way, the matrix F_{nm} is set up.

$$F_{nm} = \Sigma_j \left[B_{nj}\ \frac{(\alpha_j - \alpha^o_j)}{(\rho_m - \rho^o_m)} + \frac{(B_{nj} - B^o_{nj})}{(\rho_m - \rho^o_m)}\ \alpha_j \right] - \frac{(B_{no} - B^o_{no})}{(\rho_m - \rho^o_m)}$$

Superscripts ^{o} are functions of ρ^o_n. If F is known plastic zones are adjusted by solving equations (22). The interaction analysis is solved again for new zone lengths.

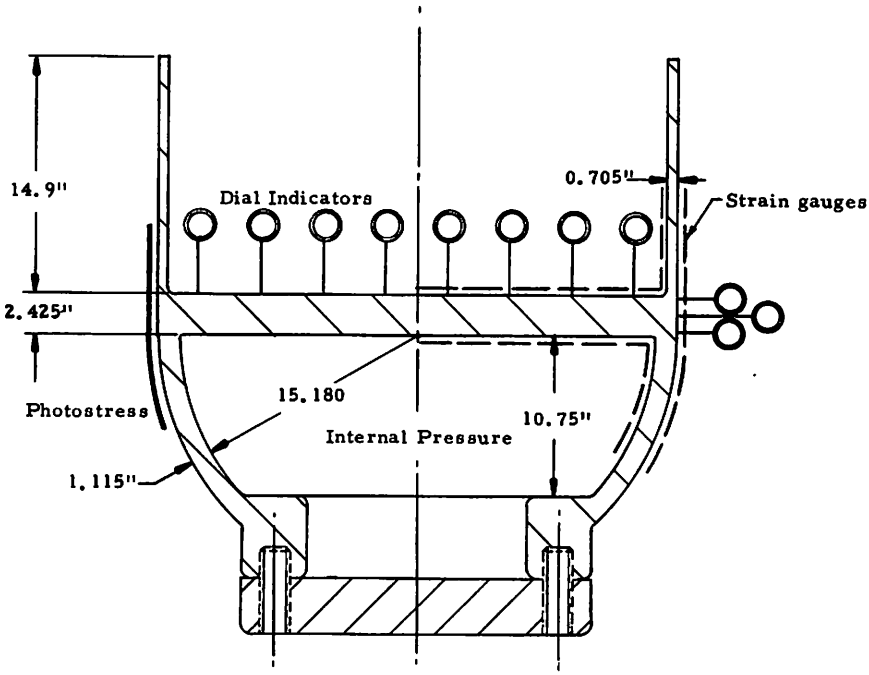

Figure 1 LIMIT TEST MODEL

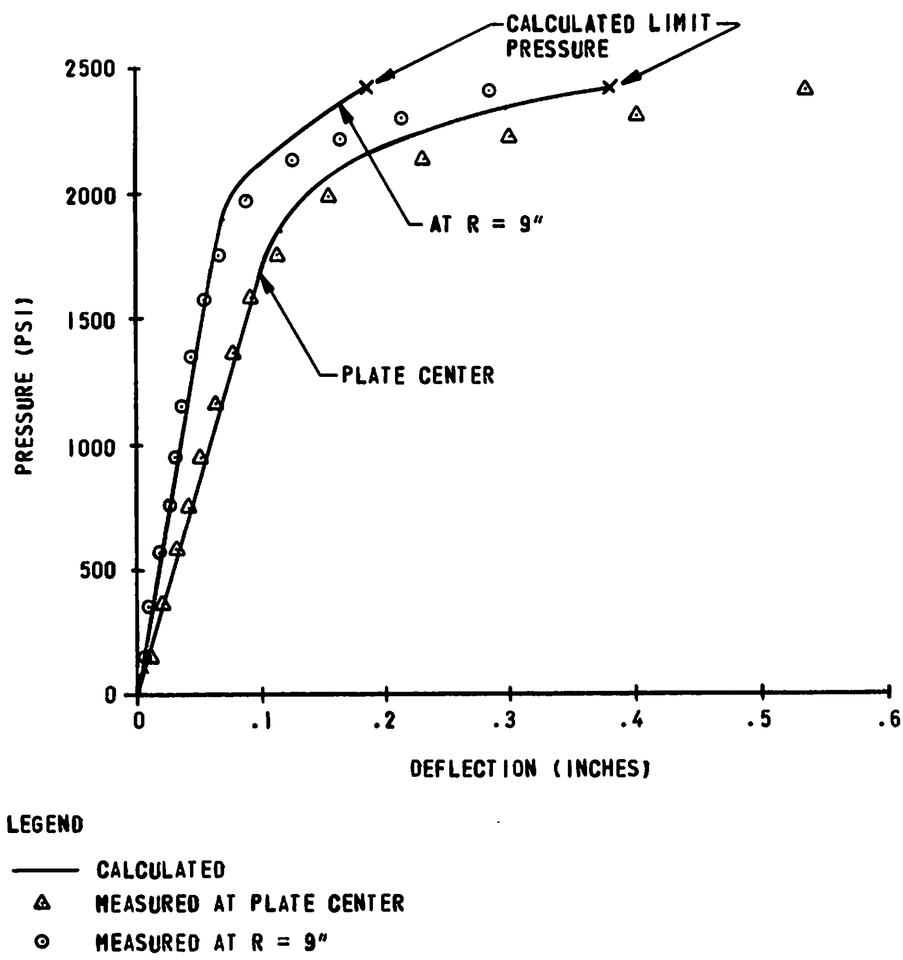

Figure 2 DEFLECTIONS OF A CIRCULAR FLAT PLATE IN TEST MODEL

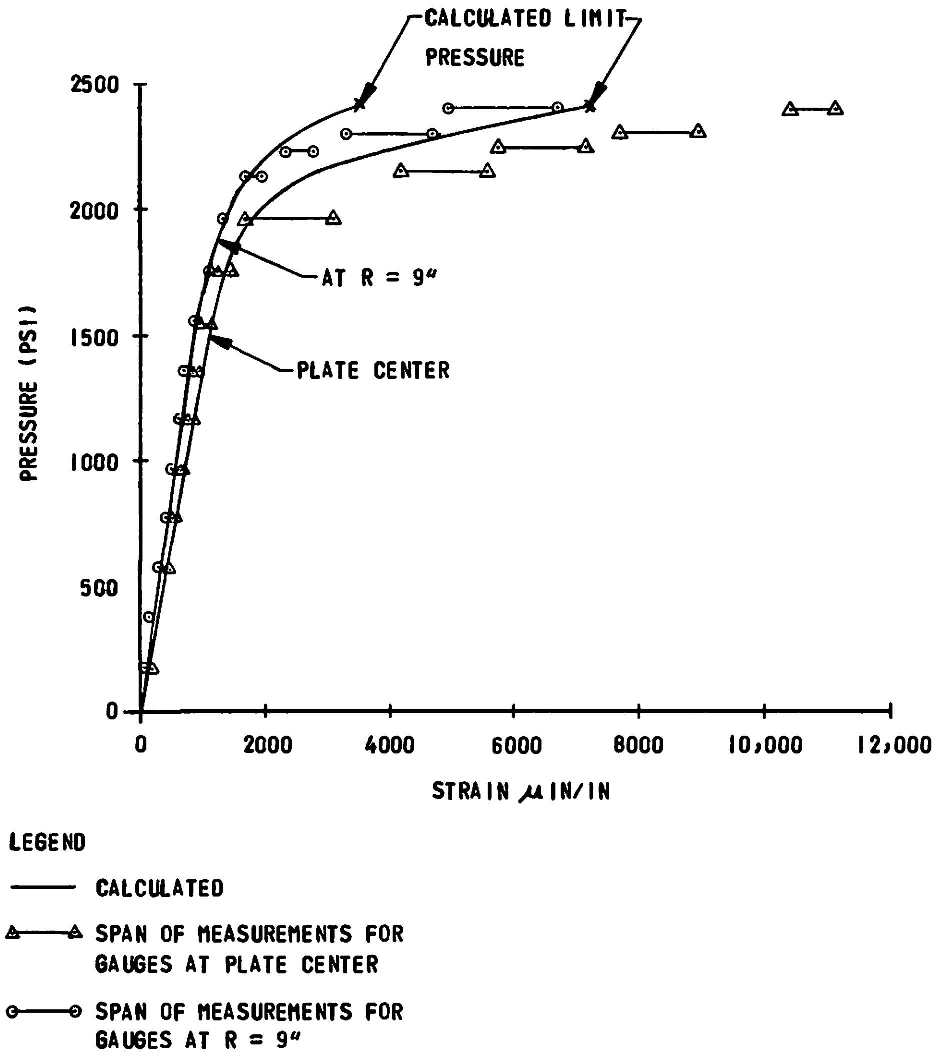

Figure 3 CIRCUMFERENTIAL STRAIN IN FLAT PLATE TEST MODEL

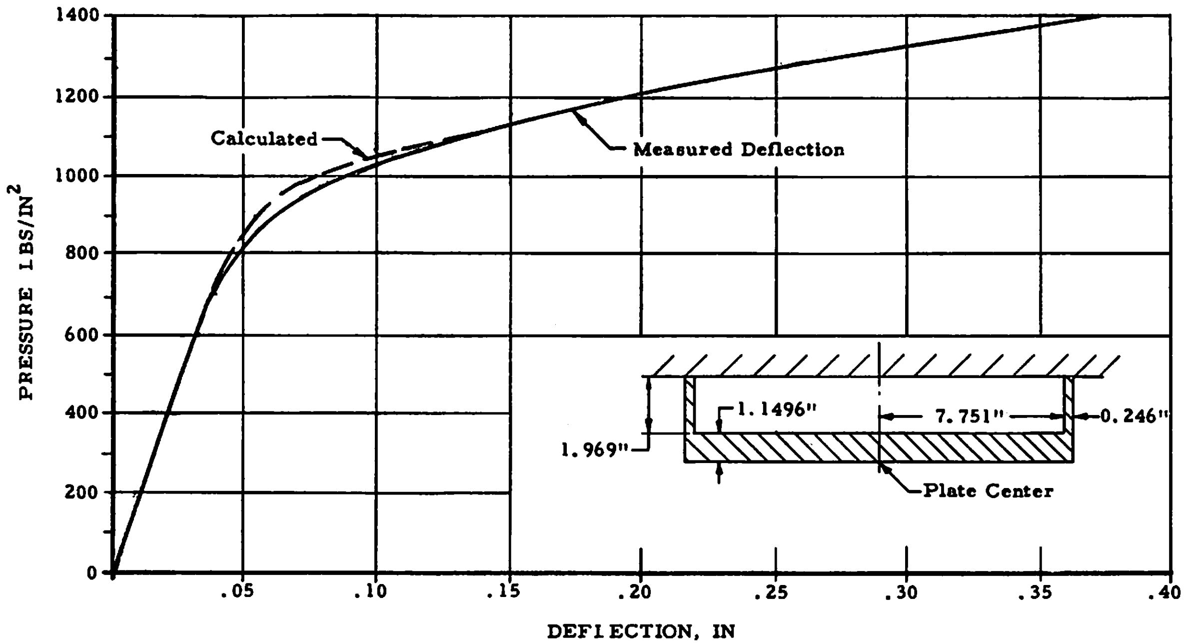

Figure 4

Deflection of Plate Center (Save' Model)

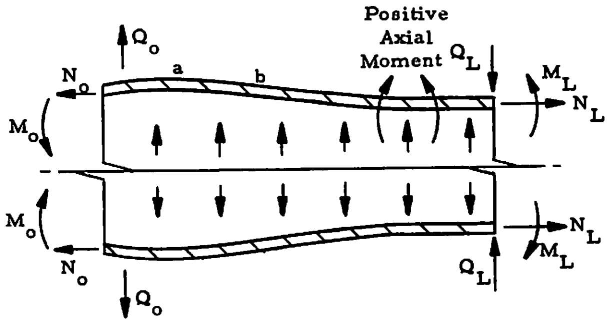

AM Elastic stress profile
CL Elastic profile with hinge at leading edge
DEK Plastic zone and hinge at leading edge
DEFGHJ Three plastic zones and hinge at leading edge

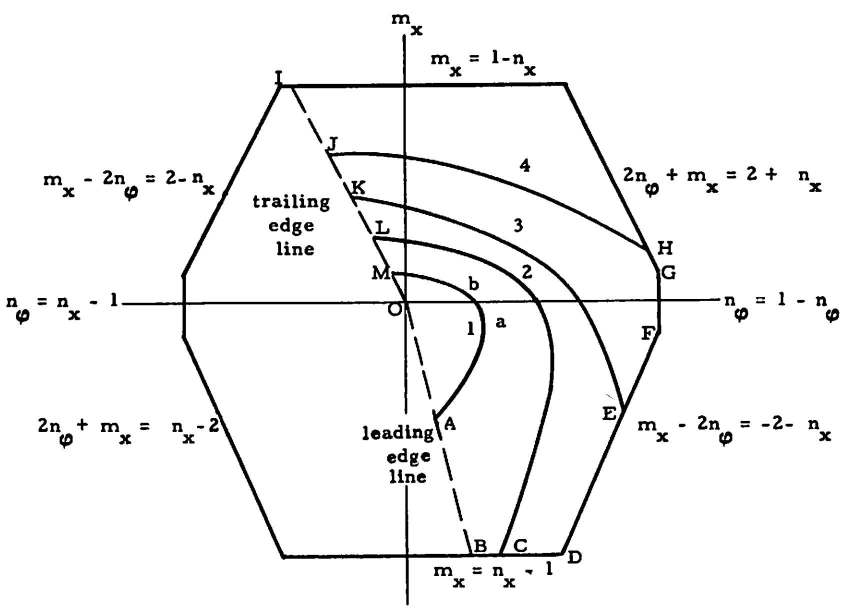

Figure 5 CYLINDRICAL SHELL YIELD POLYGON

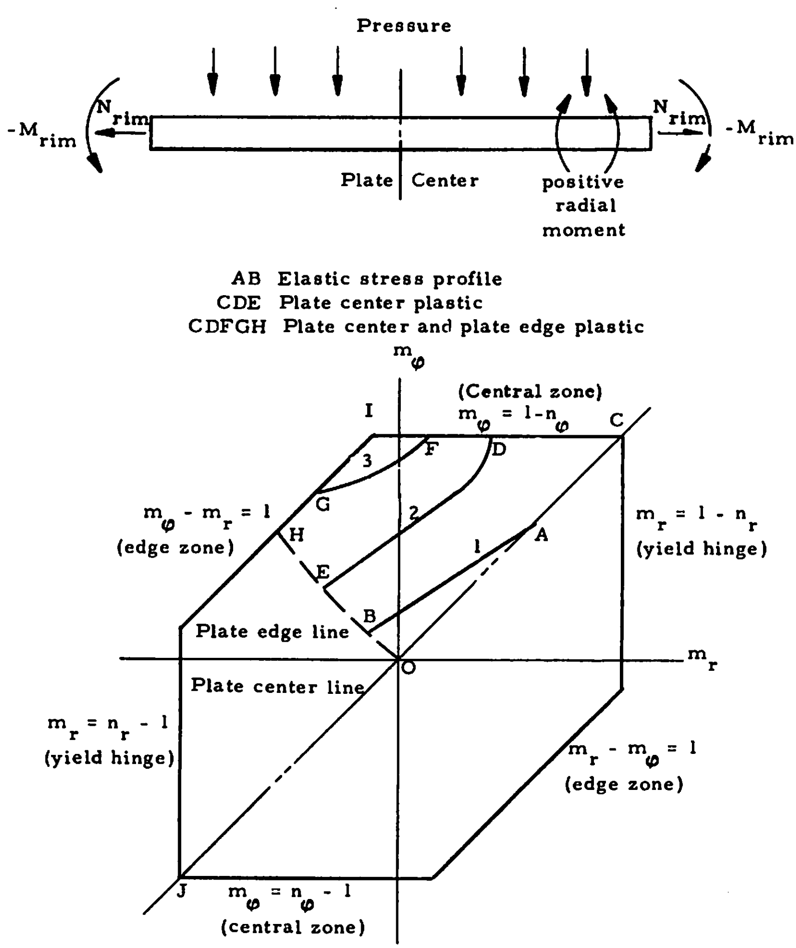

Figure 6 CIRCULAR PLATE YIELD POLYGON

DISCUSSION

Q F. ELLYIN, Canada

The agreement between theoretical and experimental result is somewhat coincidental. A limited type interaction yield surface is used which may deviate from the exact Tresca surface. In addition the effect of transversal shear force in yielding is neglected. This assumption may not be justified for thick plates and it may also introduce errors of about 20% (Ellyin, F. and Deloin R., "Effect of shear in yielding of structural members", Int. J. Struct. Solids (to appear)). It would appear that the combination of several approximation somewhat counter balance in this case, but the conclusions may not be extended to other geometries.

A J. C. NICHOLS, U. S. A.

Contrary to the impression conveyed by Dr. Ellyin, the exact Tresca yield surface was used in the development of our equations for the cylindrical shell. With respect to a flat plate the development on page 10 of our paper shows that the only assumption which causes any deviation from the Tresca yield surface is the assumption that membrane forces are small for thick plates and can be treated elastically and therefore uncoupled.
With respect to transversal shear force in yielding of the flat plate it should be noted that the largest effect in the behaviour of the structure is the development of yield hinges at the plate edge. Our work indicates that an error in the yield surface of the plate does not have a great effect on the results for the structure as a whole.
We have checked our analytical approach against experimental data from three different sources with good agreement. As more data become available we will continue to check it. In the absence of data to the contrary we consider that the analytical approach has a substantial applicability.

Q A. N. SHERBOURNE, Canada

What are the geometrical limits of plate size for which your theory is valid, recognizing the existence of shear and membrane action for thick and very thin plates ?

A J. C. NICHOLS, U. S. A.

It would take a number of tests varying the thickness of the circular flat plate relative to diameter to really establish the limits of applicability. We have checked our theory with good agreement between experimental and analytical results for two ratios of diameter to thickness. The limit test model described in the paper and model 6 tested and reported by Marcel Save in Reference (3) of the paper the diameter to thickness was approximately 12 to 1. Good agreement was also obtained for comparison with data reported in "Axisymmetric Elasto-Plastic Deformation of Circular Plates Under Combined Action of Lateral Load and Membrane Forces", Y. Ohasi, S. Murakami, Memoirs of Faculty of En-

gineering, U. Nagoya, 21:79-121 (May 1969) for a diameter to thickness ratio of 25.

Q T. ARIMAN, U. S. A.

I believe you assume that the material is perfectly plastic. I believe the assumption of strain hardening material is much more common and realistic in a number of applications. Therefore, would you please make some comments on this subject. As you may know even for a strain or work hardening material depending on the theory used in the analysis (either incremental or deformation theories of plasticity) results may differ quite a bit. Therefore, would you please tell me whether the perfectly plastic material assumption is a good one for the analysis of heat-exchanger tubes in reactors. As you indicated if you are on the conservative side by this assumption I would like to know how much you are utilizing the strength of the material. My second question is related to your governing equations for plates and shells in your analysis. From those equations one can say that your analysis is valid only for axisymmetrical problems. Is that right ?

A J. C. NICHOLS, U. S. A.

Although the authors have not utilized the strain hardening material representation, experimental results would indicate the elastic-perfectly plastic material representation to be satisfactory for the case studied. It would appear that use of the strain hardening material representation would provide a more conservative solution.

The solution was developed for the complex structure of a plate bounded by two shells at the outer edge. We would recommend analytic study and confirming experiments for the particular case of tubes in reactors. In an engineering sense, the tube sheet thickness is set by the elastic stress field limitations of the ASME Nuclear Pressure Vessel Code for operational adequacy under accident conditions and, since it does not set the material thickness, the conservative solution is satisfactory.

Finally, it should be understood that the solution presented is limited to axisymmetric problems.